ELSEVIER

www.elsevier.nl/locate/jelechem

Journal of Electroanalytical Chemistry 491 (2000) 22–29

Journal of Electroanalytical Chemistry

Scanning electrochemical microscopy Part 39. The proton/hydrogen mediator system and its application to the study of the electrocatalysis of hydrogen oxidation

Junfeng Zhou, Yanbing Zu, Allen J. Bard *

Department of Chemistry and Biochemistry, University of Texas at Austin, Austin, TX 78712, USA

Received 13 January 2000; received in revised form 16 February 2000; accepted 27 February 2000

Dedicated to Professor E. Gileadi on the occasion of his retirement from the University of Tel Aviv and in recognition of his contribution to electrochemistry

Abstract

The H^+/H_2 redox couple was investigated as a mediator system for scanning electrochemical microscopy (SECM) with proton reduction from a 0.01 M $HClO_4$ solution at a Pt tip. The feedback behavior of the mediator was examined at different substrates (Pt, Au). Unlike the one-electron outer-sphere redox couples usually used as mediators in SECM, this mediator system is sensitive to the catalytic activity of the substrate surface for hydrogen oxidation rather than the conductivity of the substrate. The catalytic oxidation of H_2 on Pt was studied during cyclic voltammetric scans of the Pt substrate with a tip close to the substrate, and the inhibition by oxygen adsorption on Pt was investigated. The quantitative H_2 oxidation rate was determined at different substrate potentials from SECM approach curves. The kinetic parameters for proton reduction and hydrogen oxidation were determined by steady-state SECM voltammograms. The inhibitory effect of anions (Br^-, I^-) and reduction products of NO_3^- for catalytic H_2 oxidation on the Pt surface was also examined.

Keywords: SECM; H_2 oxidation; Electrocatalysis

1. Introduction

Scanning electrochemical microscopy is a versatile technique that can be used to obtain topographic images of surfaces and to study the electronic conductivity and chemical activity of a substrate [1]. The SECM measurement is usually conducted in a solution containing an appropriate redox species, usually one that shows a fast Nernstian one-electron-transfer reaction, which serves as a mediator system, as shown in Fig. 1A. This figure also illustrates the instrumental setup and basic feedback principle. The tip potential is adjusted to reduce O at a diffusion-controlled rate. When the tip is far from the substrate, a steady-state current, $i_{T,\infty}$, flows. This current results from the flux of O to the electrode through hemispherical diffusion to the tip. As the tip is brought close to the substrate, i.e. within a few tip radii, the effect of feedback appears. If R generated at the tip cannot be oxidized at the substrate, negative feedback occurs due to the blocking effect of the substrate on the diffusion of O, and the tip current, i_T, is smaller than $i_{T,\infty}$. On the other hand, if the substrate electrode can oxidize R, positive feedback is established, and $i_T > i_{T,\infty}$.

In this paper, the H^+/H_2 couple was used as a mediator couple to study tip current feedback. This couple is especially convenient for SECM because the addition of no other redox species is required (Fig. 1B). The steady-state current at microelectrodes for hydrogen evolution from strong and weak acids has been studied recently [2]. The chemical step for proton discharge is usually kinetically controlled in weak acids, while a steady-state current controlled by proton diffusion is found for strong acids [2]. We report here the SECM feedback behavior of the H^+/H_2 mediator sys-

* Corresponding author. Tel.: +1-512-4713761; fax: +1-512-4710088.

E-mail address: ajbard@mail.utexas.edu (A.J. Bard).

0022-0728/00/$ - see front matter
PII: S0022-0728(00)00100-5

tem at ~10 mM concentrations of strong acid at different substrates and demonstrate that the feedback of the redox couple depends on the catalytic activity of the substrate surface for hydrogen oxidation.

The catalytic oxidation of hydrogen on platinum has received a great deal of attention and has been studied extensively [3–7], especially in connection with the use of hydrogen as a fuel-cell anode reactant. A high catalytic hydrogen oxidation rate can be obtained at an unoxidized Pt surface, while the formation of a surface oxide layer, as well as the specific adsorption of some anions, can inhibit the catalytic activity [6,7]. In this paper, the change of the SECM tip current during the cyclic voltammetry of a Pt substrate was used to demonstrate the effect of the surface oxide and anion adsorption on hydrogen oxidation. The quantitative reaction rate was obtained by fitting the SECM approach curves with theoretical ones at different substrate potentials, and the kinetic parameters of the H^+/H_2 system were measured from the steady-state voltammogram with the tip in close proximity to the substrate.

2. Experimental

2.1. Materials

All chemicals were reagent grade and were used as received. All solutions were prepared with deionized water (Milli-Q, Millipore Corp.).

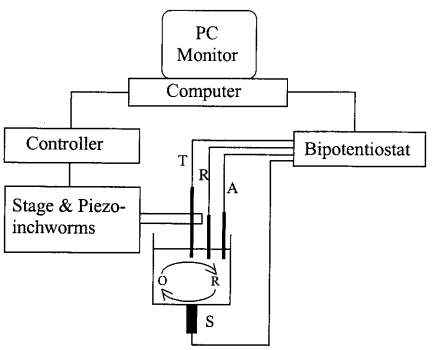

T: Tip UME, R: Reference electrode, A: Auxiliary electrode, S: Substrate electrode

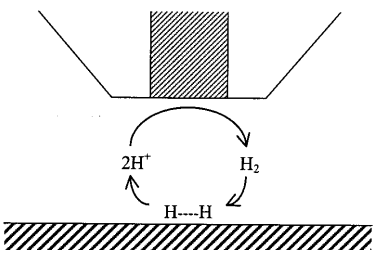

Fig. 1. (Top) Schematic illustration of SECM. (Bottom) Positive feedback of H^+/H_2 redox couple at the substrate with catalytic activity to split the H–H bond.

2.2. Electrodes

A Pt wire (25 μM diameter; Goodfellow, Cambridge, UK) was used to construct a tip ultramicroelectrode (UME) for SECM measurements. The procedure of tip preparation has been described previously [1]. The substrate Pt disk electrode had a diameter of 2.2 mm. The tip and substrate (Pt and Au) electrodes were all disk electrodes and were polished with 0.05 μm alumina, then sonicated and rinsed thoroughly with methanol and water before use. A platinum wire was used as the auxiliary electrode. The reference electrode was a saturated calomel electrode (SCE).

2.3. Electrochemical measurements

A CHI 900 SECM (CH Instruments, Austin, TX) was used for all experiments. Before each measurement, the tip and Pt substrate electrodes were cycled between −0.35 and 1.35 V versus SCE until reproducible cyclic voltammograms (CVs) were obtained. The approach curves were obtained by setting the tip potential at −0.7 V (i.e. at the diffusion limiting current for proton reduction). The approach speed of the tip to the substrate was 3 μm s^{-1}. For tip/substrate voltammograms, the tip and substrate potentials were independently controlled by the SECM bipotentiostat. The tip was brought close to the substrate (~5 μm). The tip potential was held at −0.7 V (generating hydrogen) while the substrate potential was cycled. To obtain the kinetics of the proton/hydrogen redox couple by steady-state measurements, the substrate potential was held at 0.1 V while sweeping the tip potential. The tip substrate separation, d, was varied down to 1.4 μm. All of the experiments were carried out at room temperature (r.t.).

3. Results and discussion

3.1. CV of proton on Pt microelectrodes in acid solutions with different concentrations

The tip CV in 0.01 M $HClO_4$ is shown in Fig. 2A(a). A steady-state current was obtained at potentials more negative than −0.6 V, indicating a diffusion-controlled current produced by proton reduction ($2H^+ + 2e^- = H_2$). This limiting current is given by

$$i_{T,\infty} = 4nFDca \quad (1)$$

where n is the electron transfer number (= 1 for proton reduction), F is the Faraday constant, D is the diffusion coefficient, c is the concentration of proton, and a is the radius of the tip UME. The measured current, i_T, is often normalized by $i_{T,\infty}$ and this is expressed as $I = i_T/i_{T,\infty}$.

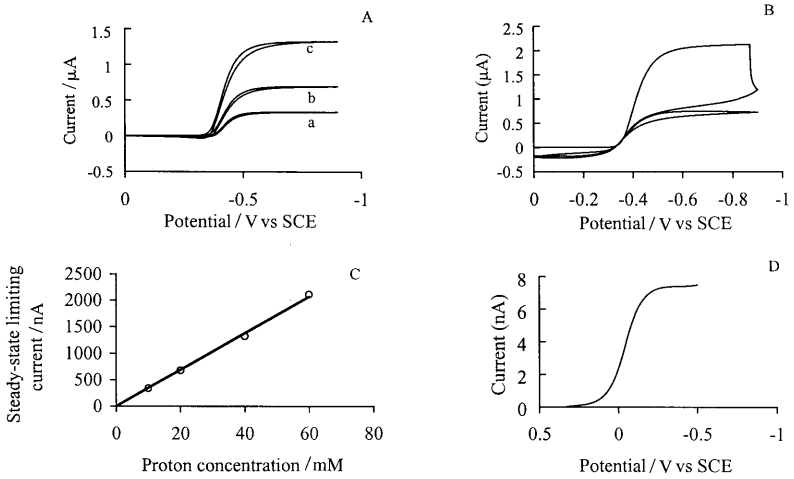

Fig. 2. Cyclic voltammetry of (A) (a) 0.01; (b) 0.02; and (c) 0.04 M $HClO_4$ and (B) 0.6 M $HClO_4$ at a 25 μm diameter Pt microelectrode in 0.1 M $NaClO_4$ aqueous solution. Scan rate was 0.1 V s^{-1}. (C) Steady state limiting current vs. $HClO_4$ concentration. (D) CV of air-saturated 0.1 M $NaClO_4$ (pH 6.1).

Hydrogen is the product of proton reduction, and at r.t., its solubility in water is 0.85 mM [8]. Thus one would expect hydrogen bubble formation at proton concentrations above about 1 mM. However, bubble formation must be nucleated, and supersaturation of hydrogen in the solution can occur. Because it is important to know the range of proton concentrations that can be used for SECM measurements before interference from bubble formation, experiments with different concentrations of the strong acid, $HClO_4$, were carried out. Fig. 2A shows the CVs for acid concentrations between 0.01 and 0.04 M. In this concentration range, there is a steady-state limiting proton reduction current with no apparent instabilities due to bubble formation, indicating that the hydrogen formed on the tip dissolved and diffused into bulk solution. When the acid concentration was increased to 0.06 M (Fig. 2B), the steady-state limiting current decreased suddenly during the scan, indicating the formation of a hydrogen bubble on the tip electrode surface. Anodic current attributable to the oxidation of the adsorbed hydrogen was observed in the potential region positive of -0.35 V versus SCE. To ensure that the SECM scans were not perturbed by bubble formation, all experiments were carried out with solutions of 0.01 M acid concentration.

The steady-state current versus proton concentration curve was linear between 0.01 and 0.06 M (Fig. 2C). A diffusion coefficient, D, of 7.1×10^{-5} cm^2 s^{-1} was calculated from the slope of the curve based on Eq. (1); this value is consistent with previously reported values [2]. The well-known high proton diffusion coefficient is due to rapid proton hopping [9].

Oxygen reduction can also occur at the tip electrode at potentials where proton reduction occurs. While solutions can be deaerated, this can be inconvenient in SECM, and it is preferable to establish conditions where deaeration is unnecessary. Fig. 2D shows the CV of the Pt tip in an air-saturated 0.1 M $NaClO_4$ aqueous solution (pH 6.1). A steady-state limiting current of 7.4 nA for the reduction of oxygen was obtained. While the position of this wave is a function of pH, the limiting current, governed by diffusion of oxygen to the tip, is independent of pH. The reduction current of 0.01 M proton is around 330 nA, which is 44 times higher than that of oxygen reduction in air-saturated solution. Thus, even without deaeration, oxygen reduction will contribute only about 2% to the total limiting current. Therefore all of the experiments were carried out without deaeration at 0.01 M acid concentrations. Note, however, that lower acid concentrations could be used, if desired, after the removal of oxygen from the solution.

3.2. H^+/H_2 mediator feedback behavior

The usual mediator systems, like $Fe(CN)_6^{3-/4-}$ can achieve positive feedback on most conductive surfaces [1]. However, the H^+/H_2 couple exhibited negative

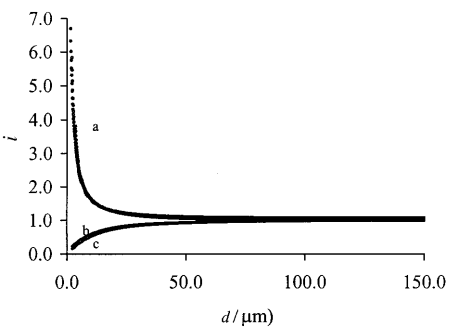

Fig. 3. SECM approach curves on (a) Pt; (b) Au; and (c) polytetrafluoroethylene substrates. Solution is 0.01 M $HClO_4 + 0.1$ M $NaClO_4$. Tip and substrate potentials were -0.7 and 0.2 V, respectively.

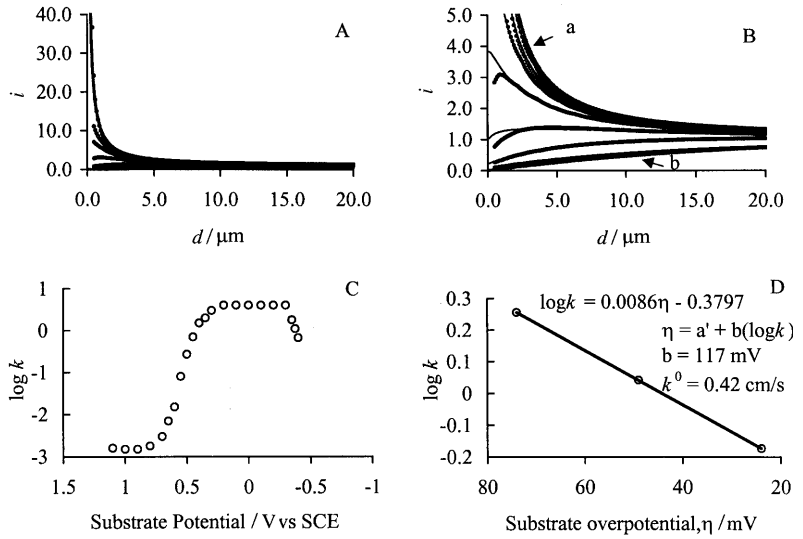

Fig. 4. (A) SECM approach curves. (B) Magnification of A. The solid lines a and b are theoretical approach curves at conducting and insulating substrates, respectively. Circle symbols are experimental approach curves and solid lines are theoretical curves at a Pt substrate with its potential held at, from top to bottom, 0, 0.4, 0.45, 0.5, 0.55, 0.6, and 1 V. (C) Heterogeneous reaction rate constant k of hydrogen oxidation at a Pt substrate with different potentials. k was obtained by fitting the experimental approach curves with the theoretical ones as shown in B. (D) Tafel plot of H_2 oxidation. Approach speed was 3 μm s^{-1}. Solution contained 0.01 M $HClO_4$ + 0.1 M $NaClO_4$.

feedback as the tip approached some conductive substrates, such as gold (Fig. 3). Since hydrogen cannot be oxidized at a non-catalytic surface, the H^+/H_2 mediator system shows the same behavior with these as with an insulating surface, and the approach curves were close to those for negative feedback with no regeneration of tip-generated species on the substrate.

When the tip approached a clean Pt surface held at a sufficiently positive potential, however, a positive feedback current appeared (Fig. 3), demonstrating rapid oxidation of hydrogen and regeneration of proton on the substrate. On a Pt surface, H_2 oxidation at r.t. is a fast process and occurs through coupled dissociation, chemisorption, and electron-transfer steps as follows [6]:

$$H_2 + 2Pt \rightarrow 2Pt(H) \quad (2)$$

$$2Pt(H) \rightarrow 2Pt + 2H^+ + 2e^- \quad (3)$$

Hydrogen oxidation at electrodes requires a catalytic surface which shows strong adsorption of H atoms and is observed only with metals like Pt, Pd, Ru, and Ir [6]. Therefore, in SECM measurements with the H^+/H_2 mediator system, positive feedback is found only with these types of metal substrates. On non-catalytic conducting or insulating surfaces, negative feedback can be expected.

3.3. Hydrogen oxidation on Pt at different potentials in $HClO_4$ — effect of Pt/O formation

When a Pt electrode is scanned to positive potentials, the formation of adsorbed oxygen-species and surface oxides occurs. The nature of the Pt surface under these conditions, which we will represent in this paper as Pt/O, depends upon the potential and has been described in terms of species like Pt_xOH, Pt_xO, and PtO_x [10–12]. These Pt/O species inhibit the catalytic activity of Pt for hydrogen oxidation [5,7]. The SECM is convenient for studying the effect of Pt surface conditions on its catalytic activity for H_2 oxidation. This was studied by two methods: SECM approach curves and tip/substrate voltammetry.

3.3.1. SECM approach curves

The SECM can be used to measure the rate constants for heterogeneous electron transfer on substrates by recording i_T versus d (the approach curve) [1]. Thus by setting the Pt tip potential to a value where diffusion-controlled proton reduction occurs (-0.7 V) and moving the tip to the Pt substrate, the H_2 oxidation rate can be extracted from the approach curve. Fig. 4A and B show approach curves at seven different substrate potentials, as well as theoretical curves for a diffusion-controlled reaction and no reaction at the substrate. In these experiments the substrate potential was held for 100 s before approaching the tip (at -0.7 V) to the substrate to achieve a stable Pt/O surface layer. By fitting the curves, the heterogeneous hydrogen oxidation rate on Pt was obtained (Fig. 4C). Note that the reaction becomes so rapid at potentials in the region of -0.3 to 0.2 V versus SCE, that the approach curves are indistinguishable from those for a diffusion-controlled reaction. In this region, the value of $i_T/i_{T,\infty}$ can be used to determine d. The smallest tip/substrate separation achieved in our experiment was 0.3 μm. At about

0.4 V versus SCE, Pt/O formation started [13] and the rate of hydrogen oxidation began to decrease. This oxidation has been proposed to proceed through stages [13]:

$$Pt + H_2O - e^- \rightarrow Pt_4OH \rightarrow Pt_2OH \rightarrow PtOH \quad (4)$$

where Pt_4OH, Pt_2OH and PtOH correspond to progressive filling of surface lattice sites in a regular array, followed by a further stage of oxidation [14]

$$PtOH - e^- \rightarrow PtO + H^+ \quad (5)$$

A specific fractional coverage of Pt/O is established rapidly at any given potential [15,16]. Above 0.7 V, the catalytic activity of the electrode surface became very low, with the approach curves being essentially those of surfaces with no regeneration capability. Between -0.3 and -0.4 V, the H_2 oxidation rate decreased with a decrease of substrate potential. Fig. 4D is a plot of the H_2 oxidation rate from the approach curves versus potential (equivalent to a Tafel plot). Over this potential range, the Tafel plot was a straight line, with a slope of 117 mV, close to a typical Tafel slope of 118 mV. The slope corresponds to a transfer coefficient, α, of 0.5 [17]. By extrapolating the line to $E = E°$, a standard reaction rate constant, k^0, of 0.42 cm s^{-1} was obtained. At substrate potentials more negative than -0.4 V, the shielding effect of the substrate on the tip current (i.e. proton reduction at the substrate) precludes the determination of kinetic parameters for hydrogen oxidation from the approach curves.

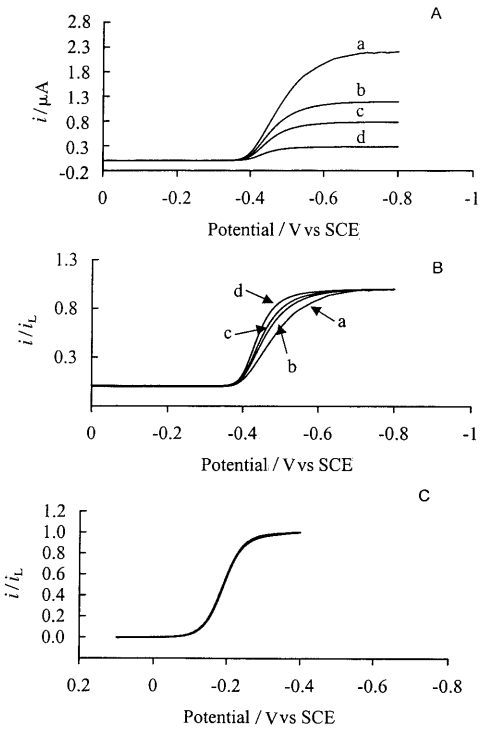

Fig. 5. (A) Tip steady-state voltammograms. (B) Normalized tip steady-state voltammograms. The tip/substrate separation was (a) 1.36; (b) 2.72; (c) 4.47; and (d) 215 μm. Scan rate was 10 mV s^{-1}. Solution was 0.01 M $HClO_4$ and 0.1 M NaCl. (C) Nine normalized tip steady-state voltammograms (overlapped with each other). The tip/substrate separations were 2.5, 3.0, 3.1, 4.0, 5.2, 7.1, 8.3, 12.7, and 25.5 μm. The solution was 5 mM $Ru(NH_3)_6^{3+}$ + 0.1 M NaCl.

Table 1
Kinetic parameters for redox of H^+/H_2 at Pt tip electrode from SECM steady-state voltammograms [a]

No.	$\Delta E_{1/4}$/mV	$\Delta E_{3/4}$/mV	L	i_T	k^0/cm s^{-1}	α
1	41.9	45.3	0.31	3.22	0.37	0.45
2	33.5	47	0.218	4.28	0.36	0.48
3	35.2	48.5	0.168	5.35	0.36	0.5
4	41	53	0.116	7.41	0.37	0.46
5	46	57	0.108	7.91	0.32	0.45

[a] $\Delta E_{1/4} = E_{1/4} - E_{1/2}$; $\Delta E_{3/4} = E_{1/2} - E_{3/4}$.

The kinetics of proton reduction at the tip were obtained by the SECM technique previously described [18–21]. Tip voltammograms were obtained at different d while holding the substrate potential at 0.1 V (Fig. 5A). Fig. 5B presents the normalized voltammograms derived from Fig. 5A, where i is the tip current and i_L is the diffusion-limited tip current. The figure shows that the voltammograms become more and more drawn out with a decrease of d. For a reaction that remains essentially Nernstian at all d, e.g. $Ru(NH_3)_6^{3+}$, the voltammograms overlap at different d (Fig. 5C). The H^+/H_2 reaction is diffusion-controlled at large d. With the decrease of d, the mass transfer coefficient, m, increased, so kinetic information can be extracted. The steady-state voltammograms were analyzed using the uniform approximation method [21]. The quartile potentials ($E_{1/4}$, $E_{1/2}$, $E_{3/4}$; the potentials at which the tip current is 1/4, 1/2, and 3/4 of i_L) were obtained from the digitized data. Based on the equation [18]:

$$i_T(E,L)/i_L = [0.68 + 0.78377/L + 0.3315\exp(-1.0672/L)]/(\theta + 1/\kappa) \quad (6)$$

where $L = d/a$, the kinetic parameter

$$\kappa = k^0 \exp[-\alpha nf(E - E°')]/m_0 \quad (7)$$

and the effective mass-transfer coefficient for SECM is

$$m_0 = 4D_0[0.68 + 0.78377/L + 0.3315\exp(-1.0672/L)]/(\pi a) \quad (8)$$

the kinetic parameters were calculated and are listed in Table 1. The average standard reaction rate constant and transfer coefficient are 0.36 cm s^{-1} and 0.47, respectively, which are similar to those measured by approach curves.

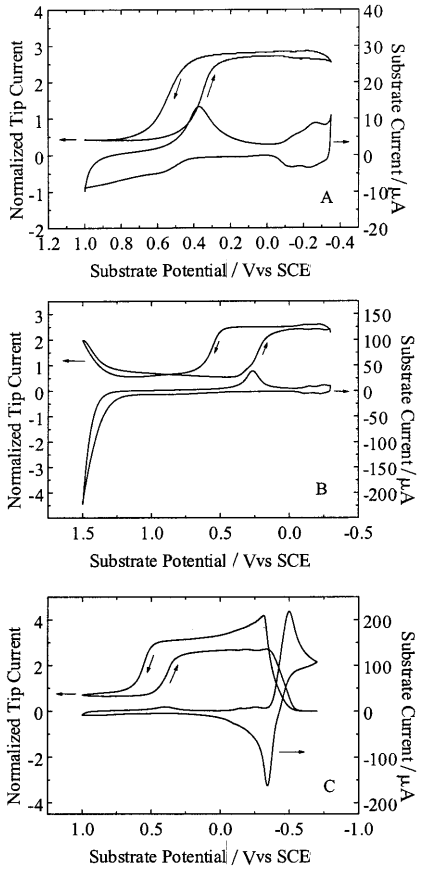

Fig. 6. Tip and substrate voltammograms in 0.01 M $HClO_4 + 0.1$ M $NaClO_4$ solution. The separation between the tip and substrate electrode was ~ 5 μm. The tip was a 25 μm diameter Pt microelectrode, and the substrate was a 2.2 mm diameter Pt electrode. Tip potential, -0.7 V. Substrate potential scan rate, 0.1 V s^{-1}. The three figures show scans across different potential regions: (A) 1.0 to -0.35; (B) 1.5 to -0.35; (C) 1.0 to -0.7 V.

3.3.2. Substrate CV with tip close to the substrate (tip/substrate voltammogram)

The effect of Pt/O formation on hydrogen oxidation can also be studied by holding the tip at a small distance from the Pt substrate (~ 5 μm) while generating hydrogen and cycling the substrate potential. A previous study of the ingress and egress of protons from a polyaniline film has been probed in this way by SECM [22] based on the fact that the tip current was also sensitive to the change of the proton concentration near the substrate surface. In the tip/substrate voltammogram measurements here, the CV of the Pt substrate and the tip feedback current were recorded simultaneously, as shown in Fig. 6. In the CV of the Pt substrate electrode, three regions can be distinguished based on the behavior of the tip held at -0.7 V.

In the hydrogen region (E_s of about 0 to -0.3 V, Fig. 6A, B), a positive tip current feedback was established. In this potential region, the adsorption and desorption of hydrogen atoms resulted in changes of proton concentration near the electrode surface and these transient effects produce slightly different currents on the forward and back scan. The smaller tip feedback current observed in the negative scan compared to that of a positive scan reflects the decrease of proton concentration due to the adsorption of hydrogen on the Pt substrate [6]:

$$H^+ + Pt + e^- \rightarrow PtH(ad) \quad (9)$$

During the desorption of hydrogen atoms from the substrate during the positive scan (the reverse process of reaction (9)), the tip current was slightly higher. Several small peaks appeared in the tip current curve corresponding to the hydrogen atom adsorption/desorption peaks in the CV of the Pt substrate. When the substrate moved to more negative potentials (Fig. 6C), proton reduction occurred, and this caused shielding of the tip and a decrease in the tip current. Hydrogen oxidation proceeded at a diffusion-controlled rate on the Pt substrate during a positive scan until potentials of about 0.4 V, where the onset of Pt/O formation occurs. The tip current dropped rapidly at potentials higher than 0.5 V. In the potential region more positive than 0.8 V (Fig. 6A, B, C), negative feedback was observed with the small tip current mainly due to the proton diffusion from bulk solution into the gap between the tip and substrate. In the reverse scan, the tip current remained small, since the surface remained covered with Pt/O until 0.3 V, where it then increased rapidly to the positive feedback value. The reduction of Pt/O at this potential, as indicated by the cathodic peak in the substrate voltammogram, produces free Pt sites that are active for hydrogen oxidation. The hysteresis observed in the tip current on scanning the substrate potential can thus be ascribed to the differences in potentials for Pt/O formation and reduction. At potentials where oxygen evolution occurs at the substrate, the tip current increased (Fig. 6B). This can be ascribed to the decomposition of H_2O producing a decrease of pH near the substrate surface and the generation of dissolved oxygen.

3.4. Hydrogen oxidation on Pt in HNO_3

Since reduction of the nitrate ion is also possible in HNO_3 solutions, somewhat different considerations apply in SECM with the H^+/H_2 couple compared to acids like $HClO_4$, HCl, and H_2SO_4. Indeed, we have used SECM to study the reduction of HNO_3 and the formation of hydroxylamine, as will be reported elsewhere [23]. Reduction of NO_3^- on Pt is inhibited by the adsorption of hydrogen [24,25], but NO_3^- can be reduced at more negative potentials. The catalytic activity of a Pt electrode for hydrogen oxidation was examined in 0.01 M HNO_3 and 0.1 M $NaNO_3$ aqueous solution by tip/substrate voltammetry (Fig. 7). The behavior observed is similar to that seen in $HClO_4$, although the

decrease in hydrogen oxidation on a positive sweep begins at somewhat less positive potentials and is somewhat more drawn out. On the reverse sweep, hydrogen oxidation starts following Pt/O reduction. A key aspect of this result is that a Pt tip held at positive potentials, like 1.1 V versus SCE, can be used to detect hydroxylamine oxidation without interference from H_2 oxidation [23].

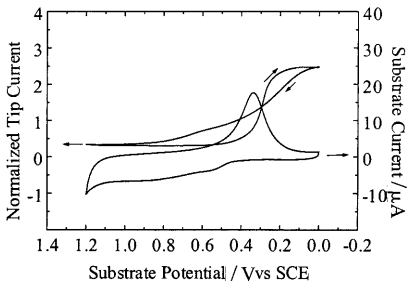

Fig. 7. Tip/substrate voltammogram in 0.01 M $HNO_3 + 0.1$ M $NaNO_3$ solution. Other parameters as in Fig. 6.

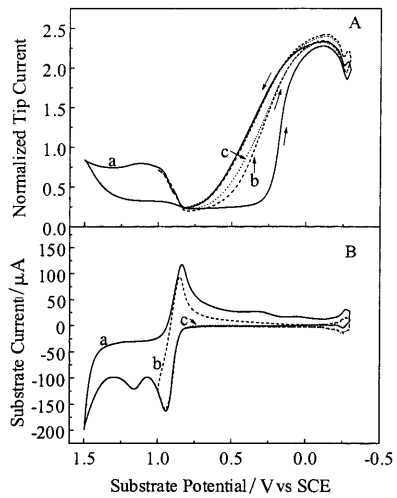

Fig. 8. (A) Tip and (B) substrate voltammograms in 0.01 M $HClO_4 +$ 0.1 M $NaClO_4 + 10$ mM KBr solution. The scanning potential regions are (a) -0.3 to 1.5; (b) -0.3 to 1.0; and (c) -0.3 to 0.8 V. Other parameters as in Fig. 6.

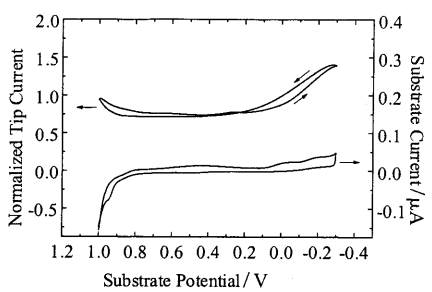

Fig. 9. Tip and substrate voltammograms in 0.01 M $HClO_4 + 0.1$ M $NaClO_4 + 0.1$ mM KI solution. Other parameters as in Fig. 6.

3.5. The effect of adsorbed Br^- and I^- on the catalytic activity of a Pt electrode

Specifically adsorbed species can affect the catalytic activity of Pt electrodes [6]. For example, previous studies have shown that halide can chemisorb on a Pt electrode surface; aqueous I^- has been shown to form an uncharged adsorbed species while Br^- is adsorbed in the anionic form [26–28]. The presence of adsorbed halide can retard hydrogen oxidation and the formation of Pt/O, because of blocking of the Pt active surface sites by halide or by changes in the electronic properties of the electrode surface. The influence of Br^- on the Pt electrode surface is shown by three tip/substrate voltammograms in Fig. 8. Fig. 8A shows the tip current ($E_T = -0.7$ V) versus substrate potential curves and Fig. 8B the simultaneous substrate voltammograms. Three different voltammograms were obtained under the same conditions, except for the positive limit in substrate potential. The solution was 0.01 M $HClO_4$, 0.1 M $NaClO_4$, and 0.01 M KBr and the substrate potential was scanned from -0.3 to 1.5, 1, and 0.8 V. The decrease in i_T at potentials more negative than -0.15 V indicates shielding by the substrate with transient effects attributable to hydrogen adsorption and desorption on the substrate. In a scan toward positive currents, i_T started to decrease at about 0.05 V, a considerably less positive potential than for the same solution in the absence of Br^- (Fig. 6). This suggests that Br^- adsorption blocks hydrogen oxidation. The tip current remained small until the onset of Br^- oxidation, when Br_2 begins to be collected at the tip. If the substrate scan was reversed at 0.8 or 1.0 V, the tip current essentially retraced that of the forward scan, although the onset of hydrogen oxidation occurred at slightly more negative E_S values. If the positive scan continued to $+1.5$ V, the tip current decreased on the back scan and hydrogen oxidation did not start again until about 0.2 V. This result suggests that Pt/O formation can occur at 1.5 V and block both Br^- and H_2 oxidation until it is reduced at 0.2 V. The effect of Pt/O shown for the scan to 1.5 V suggests the absence of Pt/O at potentials below 1.0 V and the prevention of Pt/O formation by adsorbed Br^-.

A similar experiment, but with I^- at a much lower concentration is shown in Fig. 9. As with Br^- the adsorption of iodide suppressed hydrogen oxidation and Pt/O formation. Note that I^- oxidation is not seen in these curves because of the low concentration of iodide. The blocking of hydrogen oxidation by I^- starts at even more negative potentials than with Br^- and suggests extensive coverage of the Pt substrate by adsorbed iodide, even at this low concentration.

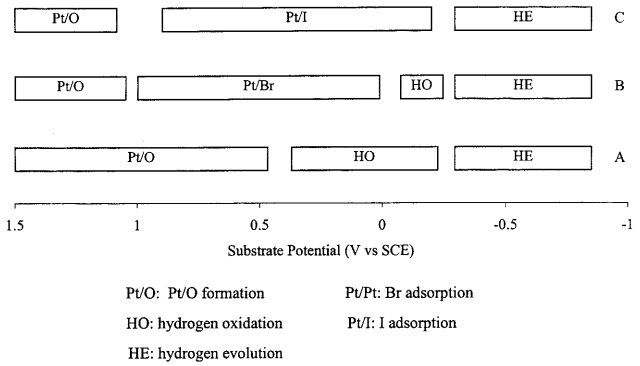

Fig. 10. Schematic demonstration of the regions of Pt surface activity with applied potential. (A) 0.01 M $HClO_4$ + 0.1 M $NaClO_4$. (B) 0.01 M $HClO_4$ + 0.1 M $NaClO_4$ + 10 mM KBr. (C) 0.01 M $HClO_4$ + 0.1 M $NaClO_4$ + 0.1 mM KI.

4. Conclusions

The H^+/H_2 system can be employed as the mediator in SECM. This is a convenient system for SECM measurements in dilute acidic solution without the addition of another redox couple to establish tip current feedback. Generally it will be used in the negative feedback mode, using proton as an electroactive species, for surfaces that do not oxidize hydrogen. In special cases it can be used to study the catalytic activity of a substrate for H_2 oxidation, where positive feedback is observed in the active region (e.g. with Pt, Pd, Ru, and Ir).

SECM with the H^+/H_2 mediator system was used to study the electrocatalysis of hydrogen oxidation at a Pt electrode in 0.01 M $HClO_4$ at different potentials in the presence of adsorbed oxygen species and oxides (Pt/O). Results are summarized in Fig. 10. On a Pt/O free surface, rapid oxidation of dissolved H_2 and a diffusion-limited approach curve was observed. At more positive potentials where Pt/O forms, H_2 oxidation was hindered and finally essentially ceased. Adsorbed Br^- and I^- on a Pt electrode surface also occupied active sites, resulting in both a shift in the potential for Pt/O formation to more positive values and a decrease in the rate of H_2 oxidation. These studies demonstrate that SECM is useful in the evaluation of the activity of a catalyst surface for hydrogen oxidation. SECM with the H^+/H_2 mediator might also be useful in the study of the reaction of H_2 with other species, such as olefins, on a catalyst surface. It should also provide an approach to studying the H^+ flux through membranes, e.g. biological or lipid bilayer membranes [29–31].

Acknowledgements

The support of this research by the National Science Foundation (CHE 9870762) and the Robert A. Welch Foundation is gratefully acknowledged.

References

[1] A.J. Bard, F.-R. Fan, M.V. Mirkin, in: A.J. Bard (Ed.), Electroanalytical Chemistry, vol. 18, Marcel Dekker, New York, 1994, pp. 243–373.
[2] S. Daniele, I. Lavagnini, M.A. Baldo, F.J. Magno, J. Electroanal. Chem. 404 (1996) 105.
[3] N.M. Markovic, S.T. Sarraf, H.AA. Gasteiger, P.N. Ross, Jr., J. Chem. Soc. Faraday Trans. (1996) 3719.
[4] J. Barber, S. Morin, B.E. Conway, J. Electroanal. Chem. 446 (1998) 125.
[5] M.W. Breiter, Electrochim. Acta 7 (1962) 601.
[6] B.E. Conway, in: S. Trasatti (Ed.), Electrodes of Conductive Metallic Oxides, Part B, Elsevier, The Netherlands, 1981, pp. 433–520.
[7] V.S. Bagotzky, N.V. Osetrova, J. Electroanal. Chem. 43 (1973) 233.
[8] R.C. Weast (Ed.), CRC Handbook of Chemistry and Physics, 67th ed., CRC Press, Boca Raton, FL, 1986.
[9] M.L. Klein, M. Parrinello, Science 275 (1997) 817.
[10] T. Biegler, D.A.J. Rand, R. Woods, J. Electroanal. Chem. 29 (1971) 269.
[11] J. Ord, F.C. Ho, J. Electrochem. Soc. 118 (1971) 46.
[12] W. Böld, M.W. Breiter, Electrochim. Acta 5 (1961) 145.
[13] H. Angerstain-Kozlowska, B.E. Conway, W.B.A. Sharp, J. Electroanal. Chem. 43 (1973) 9.
[14] S. Gilman, Electrochim. Acta 9 (1964) 1025.
[15] R. Woods, in: A.J. Bard (Ed.), Electroanalytical Chemistry, vol. 9, Marcel Dekker, New York, 1977.
[16] B.E. Conway, B. Barnett, H. Angerstein-Kozlowska, J. Chem. Phys. 93 (1990) 8361.
[17] L.R. Faulkner, A.J. Bard, Electrochemical Methods: Fundamentals and Applications, Wiley, New York, 1980, p. 106.
[18] M.V. Mirkin, T.C. Richards, A.J. Bard, J. Phys. Chem. 97 (1993) 7672.
[19] M.V. Mirkin, L.O.S. Bulhoes, A.J. Bard, J. Am. Chem. Soc. 115 (1993) 201.
[20] M.V. Mirkin, A.J. Bard, J. Electrochem. Soc. 139 (1992) 3535.
[21] M.V. Mirkin, A.J. Bard, Anal. Chem. 97 (1993) 7672.
[22] M.H.T. Frank, G. Denuault, J. Electroanal. Chem. 354 (1993) 331.
[23] L. Halaoui, A.J. Bard, H. Sharifian, in preparation.
[24] O.A. Petrii, T.Y. Safonova, J. Electroanal. Chem. 331 (1992) 879.
[25] G. Horanyi, E.M. Rizmayer, J. Electroanal. Chem. 188 (1985) 265.
[26] R.F. Lane, A.T. Hubbard, J. Phys. Chem. 79 (1975) 808.
[27] J.F. Rodriguez, J.E. Harris, M.E. Bothwell, T. Mebrahtu, M.P. Soriaga, Inorg. Chim. Acta 148 (1988) 123.
[28] G.M. Berry, M.E. Bothwell, B.G. Bravo, G.J. Cali, T. Mebrahtu, S.L. Michelhaugh, J.F. Rodriguez, M.P. Soriaga, Langmuir 5 (1989) 707.
[29] C.K. Mathews, K.E. Van Holde, Biochemistry, 2nd ed., 1992, p. 521.
[30] P. Mitchell, Science 206 (1979) 1148.
[31] P.C. Hinkle, M.A. Kumar, A. Resetar, D.L. Harris, Biochemistry 30 (1991) 3576.